

Test chamber and forensic microscopy investigation of the transfer of brominated flame retardants into indoor dust via abrasion of source materials

Rauert, Cassandra; Harrad, S.; Suzuki, G.; Takigami, H.; Uchida, N.; Takata, K.

DOI:
[10.1016/j.scitotenv.2014.06.029](https://doi.org/10.1016/j.scitotenv.2014.06.029)

License:
None: All rights reserved

Document Version
Early version, also known as pre-print

Citation for published version (Harvard):
Rauert, C, Harrad, S, Suzuki, G, Takigami, H, Uchida, N & Takata, K 2014, 'Test chamber and forensic microscopy investigation of the transfer of brominated flame retardants into indoor dust via abrasion of source materials', *Science of the Total Environment*, vol. 493, pp. 639-648.
<https://doi.org/10.1016/j.scitotenv.2014.06.029>

[Link to publication on Research at Birmingham portal](#)

Publisher Rights Statement:
Final publisher version available at: <http://dx.doi.org/10.1016/j.scitotenv.2014.06.029>

General rights

Unless a licence is specified above, all rights (including copyright and moral rights) in this document are retained by the authors and/or the copyright holders. The express permission of the copyright holder must be obtained for any use of this material other than for purposes permitted by law.

- Users may freely distribute the URL that is used to identify this publication.
- Users may download and/or print one copy of the publication from the University of Birmingham research portal for the purpose of private study or non-commercial research.
- User may use extracts from the document in line with the concept of 'fair dealing' under the Copyright, Designs and Patents Act 1988 (?)
- Users may not further distribute the material nor use it for the purposes of commercial gain.

Where a licence is displayed above, please note the terms and conditions of the licence govern your use of this document.

When citing, please reference the published version.

Take down policy

While the University of Birmingham exercises care and attention in making items available there are rare occasions when an item has been uploaded in error or has been deemed to be commercially or otherwise sensitive.

If you believe that this is the case for this document, please contact UBIRA@lists.bham.ac.uk providing details and we will remove access to the work immediately and investigate.

Manuscript Number: STOTEN-D-14-01057

Title: Test Chamber and Forensic Microscopy Investigation of the Transfer of Brominated Flame Retardants into Indoor Dust via Abrasion of Source Materials

Article Type: Research Paper

Keywords: Brominated flame retardants, HBCDs, PBDEs, Migration pathways to dust, Product abrasion, Forensic microscopy, Test chambers

Corresponding Author: Ms. Cassandra Rauert,

Corresponding Author's Institution: University of Birmingham

First Author: Cassandra Rauert

Order of Authors: Cassandra Rauert; Stuart Harrad; Go Suzuki; Hidetaka Takigami; Natsuyo Uchida; Kyouko Takata

Abstract: Brominated flame retardants (BFRs) have been detected in indoor dust in many studies, at concentrations spanning several orders of magnitude. Limited information is available on the pathways via which BFRs migrate from treated products into dust, yet the different mechanisms hypothesised to date may provide an explanation for the wide range of reported concentrations. In particular, direct transfer of BFRs to dust via abrasion of particles or fibres from treated products may explain elevated concentrations (up to 210 mg g⁻¹) of low volatility BFRs like decabromodiphenyl ether. In this study, an indoor dust sample containing a low concentration of hexabromocyclododecane, or HBCD, (110 ng g⁻¹ ΣHBCDs) was placed on the floor of an in-house test chamber. A fabric curtain treated with HBCDs was placed on a metal mesh shelf 3 cm above the chamber floor and abrasion induced using a stirrer bar. This induced abrasion generated fibres of the curtain, which contaminated the dust on the chamber floor, and ΣHBCD concentrations in the dust increased to between 4 020 and 52 500 ng g⁻¹ for four different abrasion experiment times. The highly contaminated dust (ΣHBCD at 52 500 ng g⁻¹) together with three archived dust samples from various UK microenvironments, also known to contain high concentrations of BFRs, were investigated with forensic microscopy techniques. Fibres or particles abraded from a product treated with BFRs were identified in all dust samples, thereby accounting for the elevated concentrations detected in the original dust (3 500 to 88 800 ng g⁻¹ ΣHBCD and 24 000 to 1 438 000 ng g⁻¹ for BDE-209). This study shows how test chamber experiments alongside forensic microscopy techniques, can provide valuable insights into the pathways via which BFRs contaminate indoor dust.

Suggested Reviewers: Tom Webster
Boston University
twebster@bu.edu

Jeff Wagner
California Department of Public Health
Jeff.Wagner@cdph.ca.gov

Charles Weschler

University of Medicine and Dentistry of New Jersey
weschlch@umdnj.edu

Tunga Salthammer
Fraunhofer Institute for Wood Research
tungasalthammer@wki.fraunhofer.de

Sutapa Ghosal
California Department of Public Health
Sutapa.Ghosal@cdph.ca.gov

Opposed Reviewers:



Cassandra Rauert,
Division of Environmental Health & Risk Management,
School of Geography Earth and Environmental Sciences,
University of Birmingham,
Birmingham,
B15 2TT,
UK

Tel. +44 121 414 5431

Fax +44 121 414 3078

Email c.b.rauert@bham.ac.uk

The Editor,
Science of the Total Environment

March 17, 2014

SUBMISSION OF ARTICLE “Test Chamber and Forensic Microscopy Investigation of the Transfer of Brominated Flame Retardants into Indoor Dust via Abrasion of Source Materials”

Dear Sir

I hereby submit the above paper for consideration by *Science of the Total Environment*. I believe it is ideal for publication in this journal as – amongst other things - it describes to our knowledge the first experimental evidence of BFR migration to dust via abrasion of treated products. The paper also discusses the applicability of a suit of forensic microscopy techniques for the analysis of dust contamination with BFRs.

I trust that I have submitted all the necessary information at the website, but if you require any further information in order to expedite the review process, please don't hesitate to get in touch. I look forward to hearing from you.

Best Regards

Cassandra Rauert

1 **TITLE**

2 Test Chamber and Forensic Microscopy Investigation of the Transfer of Brominated
3 Flame Retardants into Indoor Dust via Abrasion of Source Materials

5 **Authors**

6 C. Rauert^a, S. Harrad^a, G. Suzuki^b, H. Takigami^b, N. Uchida^b, K. Takata^b

8 **Affiliation**

9 ^a School of Geography Earth and Environmental Sciences, University of Birmingham,
10 Birmingham, B15 2TT, UK

11 ^b Center for Material Cycles and Waste Management Research, National Institute for
12 Environmental Studies, 16-2 Onogawa, Tsukuba, Ibaraki 305-8506, Japan

14 **Corresponding Author**

15 Cassandra Rauert

16 *Division of Environmental Health & Risk Management, Public Health Building,*

17 *School of Geography, Earth & Environmental Sciences,*

18 *University of Birmingham,*

19 *Birmingham, B15 2TT, UK*

20 *Tel +44 (0)121 414 5431*

21 *Fax +44 (0)121 414 3078*

22 *c.b.rauert@bham.ac.uk*

1
2
3
4
5
6
7
8
9
10
11
12
13
14
15
16
17
18
19
20
21
22
23
24
25
26
27
28
29
30
31
32
33
34
35
36
37
38
39
40
41
42
43
44
45
46
47
48
49
50
51
52
53
54
55
56
57
58
59
60
61
62
63
64
65

23 **Abstract**

24 Brominated flame retardants (BFRs) have been detected in indoor dust in many
25 studies, at concentrations spanning several orders of magnitude. Limited information
26 is available on the pathways via which BFRs migrate from treated products into dust,
27 yet the different mechanisms hypothesised to date may provide an explanation for the
28 wide range of reported concentrations. In particular, direct transfer of BFRs to dust
29 *via* abrasion of particles or fibres from treated products may explain elevated
30 concentrations (up to 210 mg g⁻¹) of low volatility BFRs like decabromodiphenyl
31 ether. In this study, an indoor dust sample containing a low concentration of
32 hexabromocyclododecane, or HBCD, (110 ng g⁻¹ ΣHBCDs) was placed on the floor
33 of an in-house test chamber. A fabric curtain treated with HBCDs was placed on a
34 metal mesh shelf 3 cm above the chamber floor and abrasion induced using a stirrer
35 bar. This induced abrasion generated fibres of the curtain, which contaminated the
36 dust on the chamber floor, and ΣHBCD concentrations in the dust increased to
37 between 4 020 and 52 500 ng g⁻¹ for four different abrasion experiment times. The
38 highly contaminated dust (ΣHBCD at 52 500 ng g⁻¹) together with three archived dust
39 samples from various UK microenvironments, also known to contain high
40 concentrations of BFRs, were investigated with forensic microscopy techniques.
41 These techniques included Micro X-Ray Fluorescent Spectroscopy, Scanning
42 Emission Microscopy coupled with an Energy Dispersive X-ray Spectrometer,
43 Fourier Transform Infrared spectroscopy with further BFR analysis on LC-MS/MS.
44 Using these techniques, fibres or particles abraded from a product treated with BFRs
45 were identified in all dust samples, thereby accounting for the elevated concentrations
46 detected in the original dust (3 500 to 88 800 ng g⁻¹ ΣHBCD and 24 000 to 1 438 000
47 ng g⁻¹ for BDE-209). This study shows how test chamber experiments alongside
48 forensic microscopy techniques, can provide valuable insights into the pathways via
49 which BFRs contaminate indoor dust.

50
51 **Keywords**

52 Brominated flame retardants, HBCDs, PBDEs, Migration pathways to dust, Product
53 abrasion, Forensic microscopy, Test chambers

54
55
56
57
58
59
60
61
62
63
64
65

1
2
3
4
5
6
7
8
9
10
11
12
13
14
15
16
17
18
19
20
21
22
23
24
25
26
27
28
29
30
31
32
33
34
35
36
37
38
39
40
41
42
43
44
45
46
47
48
49
50
51
52
53
54
55 **Research Highlights**

- 56 • HBCD contamination of dust via source material abrasion reproduced in test
57 chamber
58 • Fragments of plastic with elevated BDE-209 content identified in dust samples
59 • Results suggest high BFR concentrations in dust due to source material abrasion
60

61 1. Introduction

62 Brominated flame retardants (BFRs) are incorporated in numerous textile, plastic and
63 foam products with extensive indoor applications. They are incorporated into
64 consumer products in two main ways: (a) via an “additive” process where the BFR is
65 physically mixed with the molten polymer, and (b) via a “reactive” process where the
66 BFR is covalently bound to the polymer. BFRs incorporated via the additive process
67 are considered loosely bound to the product and more available for release into the
68 environment than those incorporated into materials in a “reactive” manner. Owing to
69 their extensive indoor application and their low vapour pressures that favour air-to-
70 dust partitioning, BFRs such as polybrominated diphenyl ethers (PBDEs) and
71 hexabromocyclododecane (HBCD) are ubiquitous and substantial contaminants of
72 indoor dust (Besis and Samara, 2012; Covaci et al., 2006; Harrad et al., 2010a).
73 Contact with indoor dust has thus been identified as an important human exposure
74 pathway, particularly for young children who spend extended time periods crawling
75 over surfaces and display extensive hand-to-mouth contact (Jones-Otazo et al., 2005).
76 Consequently, improved understanding of the pathways via which BFRs migrate to
77 dust from treated products can inform strategies to reduce exposure. To date however,
78 limited experimental evidence is available about such migration pathways. Currently
79 hypothesised pathways include: (1) volatilisation of BFRs from the treated product
80 with subsequent partitioning to dust; (2) abrasion via physical wear and tear of the
81 treated product (likely enhanced by UV degradation of the polymer), resulting in the
82 transfer of particles or fibres of the treated product directly to dust; and (3) transfer
83 via direct contact between the treated product and dust. Pathway (1) appears
84 particularly relevant for more volatile BFRs incorporated additively into the product,
85 and is expected to result in a homogeneous bromine distribution within the dust. In
86 contrast, pathway (2) appears more applicable to the product-to-dust migration of less
87 volatile BFRs, and/or those BFRs incorporated reactively into products. A non-
88 uniform, or heterogeneous, bromine distribution is anticipated to result from this
89 migration pathway. Finally, pathway (3) also appears more relevant for additive BFRs
90 for which migration from the product matrix to the surface and uptake by surface dust
91 occurs via sorption or other physical processes such as capillary forces. A
92 homogeneous bromine distribution is hypothesised for this pathway.

93

1
2
3
4
5
6
7
8
9
10
11
12
13
14
15
16
17
18
19
20
21
22
23
24
25
26
27
28
29
30
31
32
33
34
35
36
37
38
39
40
41
42
43
44
45
46
47
48
49
50
51
52
53
54
55
56
57
58
59
60
61
62
63
64
65

94 Emission chamber studies to date have focused largely on measurement of emissions
95 to air of BFRs and related semivolatile organic compounds (SVOCs) from treated
96 products (Rauert et al., 2014). In contrast, very few studies have investigated the
97 migration of SVOCs from products to dust, with – to the authors’ knowledge - no
98 such studies existing for BFRs. Specifically, the migration to dust of phthalates (a
99 class of SVOCs) has been simulated in test chamber experiments that investigated
100 migration pathways (1) and (3) (Clausen et al., 2004; Schripp et al., 2010). Moreover,
101 while we reported recently (Rauert et al., submitted) on test chamber experiments
102 examining volatilisation with subsequent partitioning to dust of HBCDs (pathway
103 (1)); controlled test chamber experimental studies of the migration of BFRs from
104 products to dust via pathway (2), or abrasion, have yet to be reported in the literature
105 for any SVOC.

106
107 Forensic microscopy techniques such as energy dispersive Micro X-ray fluorescence
108 spectroscopy (Micro XRFS) and scanning electron microscopy with energy dispersive
109 spectroscopy (SEM/EDS) have been utilised previously to provide information on the
110 origins of dust contamination with BFRs. Suzuki et al, (2009) used Micro XRFS to
111 map dust samples, identifying particles of high bromine content, with isolated
112 particles analysed by GC-HRMS to determine their PBDE content. In a parallel study,
113 Webster et al, (2009) utilised Micro XRFS for identification of areas of high bromine
114 content in dust samples containing high concentrations of decabromodiphenyl ether
115 (BDE-209), followed by SEM/EDS to provide compositional and morphological
116 information. However, the XRFS and SEM/EDS techniques used in these preliminary
117 studies can only confirm the existence of bromine, so additional confirmation is
118 required of the presence of BFRs. Using GC-HRMS, Suzuki et al (2009) were able to
119 identify and quantify the content of PBDEs (pg per bromine rich fragment) contained
120 within individual bromine (Br)-rich particles isolated from a dust sample, with BDE-
121 209 quantified in each isolated fragment. However, due to the uncertainty associated
122 with the gravimetric determination, the mass of the particles themselves could not be
123 measured. Subsequent studies by Ghosal and Wagner, (2013) and Wagner et al,
124 (2013) reported the use of Raman micro-spectroscopy to study Br-rich particles, after
125 identification with SEM/EDS, for non-destructive confirmation of the presence of
126 PBDEs. Collectively, studies to date have all identified in dust samples the presence
127 of particles or fibres originating from a product treated with BFRs, suspected to

128 migrate via abrasion or pathway (2). This pathway may provide an explanation for the
129 high concentrations, up to 210 mg g⁻¹ (Batterman et al., 2009), reported of the
130 relatively non-volatile BDE-209 in some dust samples.

131
132 This study for the first time mimics experimentally the abrasion of a BFR source
133 material and the subsequent migration of the abraded material into dust. The dust
134 sample generated by this experiment was analysed with a combination of forensic
135 microscopy techniques to identify the abraded material. To further show the
136 applicability of these selected microscopy techniques to providing information on
137 BFR migration pathways to dust, three ‘real’ dust samples, previously sampled from
138 indoor microenvironments in the UK and containing high levels of BFRs, were
139 analysed with the same sequence of techniques. This augmented further, the existing
140 evidence that such highly contaminated dusts are due to the presence of a small
141 proportion of fibres and/or particles abraded from BFR-treated materials.

142

143 **2. Materials and Methods**

144 *2.1. Test Chamber Experiments*

145 *2.1.2. Experimental design for investigating the abrasion migration pathway.*

146 A in-house designed and built test chamber was utilised to investigate migration
147 pathway (2). The experimental design of the chamber is illustrated in Figure 1.
148 Briefly, the chamber design consisted of a cylindrical stainless steel chamber (20 cm
149 height, 10 cm diameter), with a removable aluminium mesh shelf. In this experiment,
150 the shelf was placed 3 cm above the chamber floor and a magnetic stirrer bar, 40 mm
151 x 8 mm, (Fisher Scientific, Leicestershire, UK) placed on the shelf to mimic abrasion.
152 A piece of product treated with BFRs (the BFR source) was placed on the shelf and a
153 known mass of dust placed on a glass fibre filter (GFF), situated on the chamber floor.
154 The dust contained low concentrations of HBCDs and PBDEs (Σ HBCDs = 110 ng g⁻¹
155 and Σ PBDEs = 280 ng g⁻¹). The chamber was sealed and placed on a magnetic stirrer
156 plate, operated at 200 rotations per minute. In this way, abrasion was mimicked via
157 direct contact between the rotating stirrer bar and the treated product, with the fibres
158 and particles thus generated, falling through the mesh shelf and incorporated into the
159 dust sample below. This process was conducted at room temperature, and repeated for
160 four durations of 2, 3, 21, and 48 hours.

161

162 *2.1.3. BFR source*

163 Fabric curtains treated with technical HBCD were obtained from the National
164 Institute for Environmental Studies (NIES), Tsukuba, Japan. Concentrations of
165 HBCDs in these curtains were: 18,000 mg/kg for α -HBCD, 7,500 mg/kg for β -HBCD
166 and 17,000 mg/kg for γ -HBCD (Kajiwara et al., 2013).

168 *2.1.4. Archived dust samples*

169 Three UK dust samples were chosen for detailed analysis via forensic microscopy.
170 These samples were previously identified as containing highly elevated
171 concentrations of BDE-209 and HBCDs (Harrad et al., 2010b; Harrad et al., 2008)
172 with the concentrations listed in Table 1. Each dust originated from a different
173 microenvironment category (a residential living room, office and primary school for
174 Dusts 1, 2, and 3 respectively) however little other information was available on
175 microenvironment characteristics or putative sources for these samples.

177 *2.2. Forensic Microscopy*

178 *2.2.2. Sample Preparation for Forensic Microscopy*

179 The bulk dust sample to be examined was mixed thoroughly before use. A small
180 quantity of dust (1 mg) was evenly distributed in a monolayer, with tweezers, onto a
181 25 x 25 mm square area of double sided carbon tab attached to a glass sample plate for
182 analysis with Micro XRFS.

184 *2.2.3. Forensic Microscopy Analysis*

185 Archived and test chamber experiment-generated dust samples were mapped to locate
186 areas of high bromine content with a Micro XRFS (' μ Ray' μ EDX-1200, Shimadzu
187 Co.) equipped with a Rhodium X-ray tube and Nickel filter as the X-ray filter. The
188 instrument was operated with a tube voltage of 50 keV, tube current of 1000 μ A, and
189 beam diameter of 50 μ m as described previously, (Suzuki et al., 2009). High speed
190 bromine mapping was performed using a 0.5 second dwell time with step sizes of 50
191 μ m in the x and y-directions. Initial total sample mapping was conducted
192 continuously over the 25 x 25 mm sample area for 76 hours. To achieve more
193 accurate characterisation of specific areas and possible fragments of high bromine
194 content, areas identified as 'of interest' were remapped over smaller regions of 4 x 3
195 mm and 2 x 1.5 mm for 4.5 hours and 11 minutes respectively. Regions identified as

196 Br-rich were separated from the bulk sample and positioned on an aluminium stub for
197 further analysis. Areas and fragments were then imaged with a LEXT OLS 4100 3D
198 laser microscope (Olympus, Japan) using a 20 x magnification. SEM/EDS was
199 performed on the sample areas with a JSM-7600F Field emission SEM (JEOL, Japan)
200 equipped with a retractable backscattering electron detector and energy dispersive X-
201 ray spectrometer (EDS) analyser with silicon drift X-ray detector, with analysis
202 performed at an accelerating voltage of 20 kV. Due to the close proximity of the
203 bromine $L\alpha$ (1.480 keV) and aluminium $K\alpha$ (1.486 keV) lines, bromine was
204 confirmed by the presence of the bromine $K\alpha$ line at 11.907 keV. Because the $L\alpha$
205 peak counts were at least 1000 times higher than the background aluminium peak
206 count (from the aluminium stub), interference was considered negligible. Particles
207 identified as having high bromine content with SEM/EDS were then removed with a
208 pair of tweezers and analysed with a Nicolet Continuum Microscope connected to a
209 Nicolet 6700 Fourier transform infrared (FTIR) spectrometer (Thermo Scientific,
210 Waltham, USA) using transmission infrared microscopy, and an MCT/A detector.
211 Samples were placed in a diamond compression cell and resolution was 4 cm^{-1} over a
212 determination range of $4000\text{-}650\text{ cm}^{-1}$ with a cumulative number of 128 (77 sec).
213 Sample spectra searches were conducted with the spectral library database provided
214 with the software package (OMNIC Software, Thermo Scientific). The spectra
215 searches were conducted on the entire sample spectrum as well as separate peaks of
216 interest to identify the closest library matches (represented as a % match). Particles
217 identified as containing a close spectral match to BDE-209 were removed from the
218 ATR objective under a microscope, with a pair of tweezers and collected. All particles
219 from each dust (10 for dust 1 and 15 for dust 2) were combined prior to extraction and
220 LC-MS/MS analysis to quantify BFR content.

222 *2.3. Determination of concentrations of HBCDs and PBDEs*

223 *2.3.1 Chemicals*

224 All solvents used for extraction and analysis were of HPLC grade quality (Fisher
225 Scientific, Loughborough, UK). Standards of HBCDs (α -HBCD, β -HBCD, γ -HBCD),
226 BDE-209, labelled ^{13}C HBCDs (α -, β -, γ -), d_{18} γ -HBCD and labelled ^{13}C BDE-209
227 and ^{13}C BDE-100 were acquired from Wellington Laboratories (Guelph, ON,
228 Canada). Florisil (60-100 mesh) and silica gel (60\AA , 60-100 mesh) were provided
229 from Sigma Aldrich (Dorset, UK) with concentrated sulfuric acid obtained from

230 Merck (Darmstadt, Germany). Glass fibre filters (GFF, 12.5 cm diameter, 1 µm pore
231 size, Whatman, UK) were purchased from Agilent (UK).

232

233 2.3.2 Sample analyses

234 Dust samples generated by test chamber experiments and particles identified by FTIR
235 as containing BFRs were extracted and analysed using modified in-house methods
236 (Abdallah et al, 2008, 2009). A detailed description is provided as supplementary
237 data. Briefly, samples were spiked with ¹³C-HBCD and PBDE analogues as internal
238 (surrogate) standards prior to pressurised liquid extraction (ASE, Dionex Europe, UK,
239 ASE 350) with hexane:dichloromethane (1:1 v/v). After clean-up of the crude extracts
240 via elution through sulfuric acid-impregnated silica (44% w/w), the eluates were
241 evaporated and made up to 100 µL using d₁₈ γ-HBCD and ¹³C BDE-100 in methanol,
242 as recovery determination (or syringe) standards. Analysis was conducted with a dual
243 pump Shimadzu LC-20AB Prominence liquid chromatograph (Shimadzu, Kyoto,
244 Japan) equipped with a SIL-20A autosampler, and a DGU-20A3 vacuum degasser.
245 Mass spectrometric analysis was performed using a Sciex API 2000 triple quadrupole
246 mass spectrometer (Applied Biosystems, Foster City, CA) equipped with an APPI
247 (PBDEs) or ESI (HBCDs) ion source, operated in negative ion mode.

248

249 3. Results

250 3.1. Test chamber abrasion experiments

251 Stirrer bar-induced abrasion in the test chamber was successful, with loosened fibres
252 observed post-experiment on both the tested curtain and visible fibres in the dust on
253 the chamber floor. The entire dust sample including all abraded fibres was extracted
254 and analysed to determine concentrations of HBCDs. Figure 2 shows the pre- and
255 post-experimental concentrations of HBCD diastereomers in dust for four replicates
256 of this experiment. All four experiments were run for different time periods (2, 3, 21
257 and 48 hours for experiments 1, 2, 3 and 4 respectively). However, although there is a
258 two orders of magnitude increase in concentrations of HBCDs post-experiment in all
259 cases; there is no clear relationship between the concentration in the dust and the
260 duration of the abrasion experiment. The large concentration increase is consistent
261 with the hypothesis that curtain fibres (of high HBCD concentration) have been
262 incorporated into the dust. Other experiments in the same test chamber examining
263 transfer of HBCDs via volatilisation from the same HBCD-treated curtains with

1
2
3
4
5
6
7
8
9
10
11
12
13
14
15
16
17
18
19
20
21
22
23
24
25
26
27
28
29
30
31
32
33
34
35
36
37
38
39
40
41
42
43
44
45
46
47
48
49
50
51
52
53
54
55
56
57
58
59
60
61
62
63
64
65

264 subsequent deposition to the same dust (Rauert et al., submitted) reported much lower
265 concentrations in chamber dust post experiment (average 610 ng Σ HBCDs/g), adding
266 further weight to the hypothesis that different migration pathways may result in
267 varying BFR concentrations in dust. The variable HBCD concentrations in these
268 abrasion experiments is consistent with the abrasion of treated products in indoor
269 microenvironments as ‘wear and tear’ of a product will not be uniform and will
270 depend on factors such as: the product material (e.g. plastic or fabric), how and how
271 often the product is used, as well as its age and extent to which it is exposed directly
272 to UV light and consequent weathering. The abrasion induced in these test chamber
273 experiments is highly intensive (forced), so does not represent realistic abrasion from
274 e.g. 48 hour use of a curtain. However, the results may be interpreted as an
275 acceleration test to mimic long-term abrasion. For example, if we assume 10 seconds
276 daily movement/wear and tear of the fabric from opening and closing curtains, then
277 the 2 hour chamber abrasion experiment may represent house dust concentration
278 increment from abrasion over 720 days. Abrasive contact with other fabrics such as
279 sofa covers, will likely be far more frequent, and our range of experimental durations
280 may be viewed as reflecting abrasion of a variety of domestic and commercial fabrics.
281 The ease with which abrasion can be replicated in these chamber experiments,
282 suggests this is a feasible migration pathway. The highest concentration (48 hour
283 abrasion) dust sample was analysed further with forensic microscopy techniques.

284

285 *3.2. Microscopy analysis of the chamber generated dust sample*

286 The Micro XRF identified fibres of high bromine content in the dust sample, and
287 these were analysed in closer detail using the SEM for elemental confirmation. Figure
288 3 presents the SEM backscattering image of a series of intertwined fibres and the EDS
289 elemental profile, confirming the presence of bromine via the presence of both the $K\alpha$
290 and $L\alpha$ bromine spectral lines. The fibre was isolated and analysed on the FTIR for
291 compositional information, with an 88% match returned for the polyester spectrum
292 when searching the entire sample spectrum through the library. Peaks of interest in the
293 sample spectrum were searched separately to increase the confidence of the match
294 with the reference spectrum (in particular the strong stretch at $\sim 1700\text{ cm}^{-1}$,
295 representative of a C=O double bond stretch, and weak stretches around 3000 cm^{-1} ,
296 representative of alkyl group stretches) and a 97% match for polyester was returned,

1 297 strongly suggesting the base polymer of these curtain fibres is a polyester. The HBCD
2 298 spectrum was not distinguishable however, as the HBCD concentration in the curtain
3 299 was below the LOD of the FTIR (5% HBCD content). Figure 4 shows the FTIR
4 300 spectra of the fibre, alongside reference spectra of the polyester match, and the
5 301 technical HBCD formulation for comparison. The limits of detection of the FTIR in
6 302 particular, did not allow confirmation of HBCDs in identified fibres in this sample.
7 303 However, the presence of Br-rich fibres were confirmed, suggesting the fibres
8 304 originated from the HBCD treated curtain and demonstrating the applicability of these
9 305 methods for identifying particles/fibres of high Br and high BFR content. To
10 306 investigate this applicability further, three 'real' indoor dust samples were
11 307 investigated with the same combination of methods, to determine if BFR-containing
12 308 particles/fibres could be identified in high concentration dust samples.
13
14
15
16
17
18
19
20
21
22

23 310 *3.3. Archived dust samples*

24 311 *3.3.2. Forensic Microscopy investigation*

25 312 All three archived dusts were analysed with the Micro XRFS in triplicate. Areas
26 313 containing high bromine content and bromine rich particles were identified in all
27 314 samples with 2 to 10 bromine rich fragments per mg dust. Similarly, the study by
28 315 Ghosal and Wagner, (2013) also reported ≤ 10 fragments per mg of analysed dust
29 316 sample. As the incident X-ray excitation beam is a 50 μm square area, the mapping
30 317 image provides an average of the bromine content in the sample rather than
31 318 identification of individual bromine rich fragments. Moreover, particles smaller than
32 319 50 μm may be missed, creating a selection bias with this method, and requiring
33 320 further SEM/EDS analysis for bromine confirmation. The bromine rich particles
34 321 identified in these samples ranged in size from 30 to 260 μm in length; however, it is
35 322 possible larger fragments may have fractured during dust collection preparation
36 323 techniques (vacuuming, sieving etc) or during application of the dust to the double
37 324 sided carbon tab. Figure 5 presents the Micro XRFS optical images and bromine
38 325 mapping images of typical sample areas containing bromine rich fragments. Again,
39 326 identified areas of interest (1 x 1 mm) were removed and placed on an aluminium stub
40 327 for further analysis. The areas and suspected Br-rich fragments were examined with a
41 328 laser microscope to provide detailed optical and 3D laser images. All fragments were
42 329 visually different from the surrounding dust particles having a white or slightly yellow
43 330 colouring and sharp edges, suggesting they may be pieces of a fractured polymer
44
45
46
47
48
49
50
51
52
53
54
55
56
57
58
59
60
61
62
63
64
65

1
2
3
4
5
6
7
8
9
10
11
12
13
14
15
16
17
18
19
20
21
22
23
24
25
26
27
28
29
30
31
32
33
34
35
36
37
38
39
40
41
42
43
44
45
46
47
48
49
50
51
52
53
54
55
56
57
58
59
60
61
62
63
64
65

331 rather than typical dust organic matter. Following the imaging, SEM analysis
332 performed in backscattering mode and followed by EDS was conducted on the
333 suspect Br-rich fragments, confirming the presence of bromine in all identified
334 fragments as well as the presence of antimony. The particles were not coated before
335 SEM/EDS to prevent interference with the subsequent FTIR analysis, and as a result
336 there was a charging effect on the images. However, in backscattering mode, clear
337 regions of bromine and antimony (located in the imaged bright areas) were observed
338 over the particle surface and confirmed with EDS. Due to the charging effect and the
339 uneven topography of the sample surface, quantitative elemental analysis was not
340 possible; rather the SEM qualitatively identified the presence of these elements.
341 Bromine and antimony were observed in distinct pockets on each particle surface in a
342 heterogeneous fashion, similar to the study by Wagner et al, (2013) who observed
343 clear pockets of bromine on particle surfaces. Figure 6 shows the backscattering
344 electron images of particles from all three dusts and the related EDS profiles,
345 confirming the presence of bromine and antimony. The high bromine content areas
346 originally identified with the Micro XRFS, were all shown to be associated with
347 distinct individual particles and a homogeneous bromine distribution over dust
348 particles was not seen, a result consistent with migration via pathway (2), rather than
349 pathway (1). After SEM/EDS analysis, these identified individual particles were
350 removed from the sample area with a pair of tweezers for FTIR analysis. All particles
351 identified in dust 3 were < 50 μm long and too small for removal, thereby preventing
352 further FTIR analysis. Hence in dust 3, it was only possible to confirm the presence of
353 bromine in the particles.
354
355 Eight particles from dust 1 and nine particles from dust 2 were analysed and all
356 fragments from the same dust sample had very similar spectra, suggesting a common
357 source. Library database searches of the spectra obtained from particles in dust 1 were
358 obtained to identify closest component matches from the database. Firstly the entire
359 spectrum was analysed for the top 3 matches in the database that combined, most
360 closely matched the spectrum. An 88% match was found for the combination of BDE-
361 209, antimony trioxide and an acrylic based industrial coating. To improve the
362 accuracy of the spectral matches, individual peaks and areas of interest in sample
363 spectra were run separately through the software to find the top match in the database
364 for each peak/area. The absorption spectrum in the range of 900 to 1400 cm^{-1} (often

1
2
3
4
5
6
7
8
9
10
11
12
13
14
15
16
17
18
19
20
21
22
23
24
25
26
27
28
29
30
31
32
33
34
35
365 due to C-O bond stretches, particularly from ethers) returned a 95% confidence match
366 with BDE-209, while the strong absorption at $\sim 700\text{ cm}^{-1}$ (possibly from a Sb-O bond
367 stretch) combined with the broad absorption at $3100\text{-}3500\text{ cm}^{-1}$ (from a Sb=O stretch)
368 returned a 91% match for antimony trioxide. To identify the product polymer, the
369 strong absorbance at $\sim 1750\text{ cm}^{-1}$ (often from a C=O, or C=N stretch) combined with
370 the absorbance at $2800\text{-}3000\text{ cm}^{-1}$ (often from various C-H bond stretches) returned a
371 98% match for a styrene acrylic. The same method was applied for spectra from
372 particles in dust 2 with a 73% match obtained for the combination of BDE-209,
373 antimony trioxide, and again an acrylic based industrial coating. Once more,
374 comparison of individual peaks/areas resulted in higher confidence level matches with
375 a 92% match for BDE-209, a 90% match for antimony trioxide, and a 94% match for
376 an acrylic copolymer from the strong absorbance at $\sim 1750\text{ cm}^{-1}$ and absorbance at
377 $2800\text{-}3000\text{ cm}^{-1}$. By investigating the spectral peaks/areas separately, the confidence
378 of spectral matches with database spectra was improved greatly. The lower accuracy
379 for the matched total spectrum from dust 2, is largely due to the presence of the extra
380 broad peak at 1500 cm^{-1} , reducing confidence in the accuracy of the matches. This
381 peak was similar to the broad peak seen in the reference calcium carbonate spectra,
382 suggesting calcium carbonate may have been used as a resin filler in the polymer
383 fragments isolated from dust 2.

384
385 The reference spectra for the acrylic copolymer, styrene acrylic and for an
386 acrylonitrile-butadiene-styrene (ABS) copolymer are all similar, and hence are all
387 possible matches for the polymer in the isolated fragments. ABS plastic was
388 compared, as it is commonly flame-retarded with both BDE-209 and antimony
389 trioxide, and it is thus plausible that the fragments may have originated from a source
390 containing BDE-209 treated ABS plastic. Figure 7 presents the spectra, and software
391 library database matches, for particles from dusts 1 and 2.

392
393 The limitations with these methods, primarily the high LODs of the instruments,
394 constrain these analyses to dust with very high concentrations of BFRs. The Micro
395 XRFS detects bromine concentrations $\geq 0.1\%$ in high speed mapping mode (0.5 sec
396 dwell time) (Suzuki et al., 2009), and will identify with a high degree of confidence,
397 high Br concentrations from fragments $> 50\text{ }\mu\text{m}$ in length. Smaller fragments may not
398 be identified, introducing a selection bias to this method, which is thus only suitable

1
2
3
4
5
6
7
8
9
10
11
12
13
14
15
16
17
18
19
20
21
22
23
24
25
26
27
28
29
30
31
32
33
34
35
36
37
38
39
40
41
42
43
44
45
46
47
48
49
50
51
52
53
54
55
56
57
58
59
60
61
62
63
64
65

399 for identifying Br-rich particles of Br content $\geq 0.1\%$ and particle length $> 50 \mu\text{m}$ (for
400 this particular instrument). The LOD of the FTIR introduces further limitations to
401 these methods, as the FTIR will only distinguish a BFR spectrum from the
402 particle/fibre spectrum if present at $> 5\%$ BFR content. As seen with the analysis of
403 the dust generated from abrasion of the HBCD curtain, where HBCDs were not
404 identified with the FTIR in the isolated fibres, this is a restriction on successfully
405 identifying BFRs in contaminated dust samples. Particle size is also a consideration
406 with FTIR analysis, as particles need to be separated from the sample matrix for
407 individual analysis with the diamond ATR objective. In this analysis, particles > 65
408 μm were successfully removed and analysed on the FTIR, with smaller particles (e.g.
409 from dust 3) unable to be isolated using the present methods. This again created a
410 selection bias in particles that could be analysed for the presence of BFRs, the resin
411 material and other additives in the particle. The SEM/EDS, although providing a more
412 specific elemental analysis than the Micro XRFS, is only a qualitative measure of
413 bromine (and other element) content. The uneven topography of the dust sample
414 creates difficulties for the detector to receive an accurate signal and the charging
415 effect (caused by an excess of electrons, normally minimised by carbon or platinum
416 coating of the sample) also reduces accuracy of any quantitative measurement, hence
417 this method can only be used to identify the presence of certain elements.
418 Furthermore, the SEM spectral lines for bromine and aluminium interfere, so a high
419 bromine content and the presence of the $K\alpha$ bromine line is needed for confirmation.
420 Similarly, the antimony $L\alpha$ and calcium $K\alpha$ lines interfere, providing difficulties in
421 identifying these elements unless one (antimony) is present at a much higher
422 concentration.

423 424 *3.3.3. Analysis of BFR concentration in isolated particles*

425 As many BFR containing particles as possible (10 and 15 from dust 1 and 2
426 respectively), were collected and combined for determination of BDE-209 content.
427 Table 1 lists the mass of BDE-209 (ng) quantified in the combined particles removed
428 from each dust sample. On average, the particles removed in dust sample 1 were
429 much smaller than in dust 2, and more particles were successfully removed from dust
430 2. The combination of these factors means that the total particle mass analysed in the
431 particles isolated from dust 2 was much greater, explaining the higher BDE-209
432 content quantified in the isolated particles from this dust. As with previous studies

1
2
3
4
5
6
7
8
9
10
11
12
13
14
15
16
17
18
19
20
21
22
23
24
25
26
27
28
29
30
31
32
33
34
35
36
37
38
39
40
41
42
43
44
45
46
47
48
49
50
51
52
53
54
55
56
57
58
59
60
61
62
63
64
65

433 highlighted earlier, an accurate mass measurement could not be determined for the
434 isolated particles, and hence the BDE-209 masses given can only confirm its very
435 strong presence in these particles.

437 **4. Conclusions**

438 Abrasion of a HBCD treated curtain was successfully induced in a test chamber with
439 forensic microscopy techniques identifying fibres of high bromine content throughout
440 dust samples impacted by such induced abrasion. Application of these microscopic
441 techniques to ‘real’ indoor dust samples displaying highly elevated concentrations of
442 BDE-209, identified 2 to 10 bromine rich fragments per mg dust. These fragments
443 were also identified as polymeric in origin and to contain elevated masses of BDE-
444 209. Combined, this evidence suggests strongly that the highly elevated
445 concentrations in these dust samples is due to the presence of such fragments that
446 presumably arise via abrasion of friable polymeric material. Although these
447 techniques are limited to the study of dust samples containing very high
448 concentrations of BFRs; in this study they have shown that the abrasion migration
449 pathway is a likely source of the elevated concentrations of BFRs detected in such
450 indoor dust samples. This study raises questions about dust sampling and preparation
451 techniques. Bromine rich particles, confirmed to contain BDE-209, of up to 260 µm in
452 size were detected in this study, hence sample preparation techniques that sieve bulk
453 dust samples to a particle size < 250 µm may potentially underestimate BFR
454 concentrations in that dust sample. Moreover, the heterogeneity of the distribution of
455 BFR-rich particles in the dust samples studied here, implies obtaining a representative
456 subsample of such dusts for analysis is problematic. Consequently, analysis of
457 replicate subsamples may be required to obtain an accurate picture of the BFR
458 concentration in dust from such microenvironments.

460 **5. Acknowledgements**

461 The research leading to these results has received funding from the European Union
462 Seventh Framework Program (FP7/2007-2013) under grant agreement No 264600
463 (INFLAME project).

465 **References**

- 1
2 466 Abdallah, M.A.-E.; Harrad, S.; Covaci, A. Isotope Dilution Method for Determination
3 467 of Polybrominated Diphenyl Ethers Using Liquid Chromatography Coupled to
4 468 Negative Ionization Atmospheric Pressure Photoionization Tandem Mass
5 469 Spectrometry: Validation and Application to House Dust. *Analytical*
6 470 *Chemistry*. 81:7460-7467; 2009
- 7
8 471 Abdallah, M.A.-E.; Ibarra, C.; Neels, H.; Harrad, S.; Covaci, A. Comparative
9 472 evaluation of liquid chromatography-mass spectrometry versus gas
10 473 chromatography-mass spectrometry for the determination of
11 474 hexabromocyclododecanes and their degradation products in indoor dust.
12 475 *Journal of Chromatography A*. 1190:333-341; 2008
- 13
14 476 Batterman, S.A.; Chernyak, S.; Jia, C.; Godwin, C.; Charles, S. Concentrations and
15 477 Emissions of Polybrominated Diphenyl Ethers from U.S. Houses and Garages.
16 478 *Environmental Science & Technology*. 43:2693-2700; 2009
- 17
18 479 Besis, A.; Samara, C. Polybrominated diphenyl ethers (PBDEs) in the indoor and
19 480 outdoor environments: A review on occurrence and human exposure.
20 481 *Environmental Pollution*. 169:217-229; 2012
- 21
22 482 Clausen, P.A.; Hansen, V.; Gunnarsen, L.; Afshari, A.; Wolkoff, P. Emission of Di-2-
23 483 ethylhexyl Phthalate from PVC Flooring into Air and Uptake in Dust:
24 484 Emission and Sorption Experiments in FLEC and CLIMPAQ. *Environmental*
25 485 *Science & Technology*. 38:2531-2537; 2004
- 26
27 486 Covaci, A.; Gerecke, A.C.; Law, R.J.; Voorspoels, S.; Kohler, M.; Heeb, N.V.; Leslie,
28 487 H.; Allchin, C.R.; de Boer, J. Hexabromocyclododecanes (HBCDs) in the
29 488 Environment and Humans: A Review. *Environmental Science & Technology*.
30 489 40:3679-3688; 2006
- 31
32 490 Ghosal, S.; Wagner, J. Correlated Raman micro-spectroscopy and scanning electron
33 491 microscopy analyses of flame retardants in environmental samples: a micro-
34 492 analytical tool for probing chemical composition, origin and spatial
35 493 distribution. *Analyst*. 138:3836-3844; 2013
- 36
37 494 Harrad, S.; de Wit, C.A.; Abdallah, M.A.-E.; Bergh, C.; Björklund, J.A.; Covaci, A.;
38 495 Darnerud, P.O.; de Boer, J.; Diamond, M.; Huber, S.; Leonards, P.;
39 496 Mandalakis, M.; Östman, C.; Haug, L.S.; Thomsen, C.; Webster, T.F. Indoor
40 497 Contamination with Hexabromocyclododecanes, Polybrominated Diphenyl
41 498 Ethers, and Perfluoroalkyl Compounds: An Important Exposure Pathway for
42 499 People? *Environmental Science & Technology*. 44:3221-3231; 2010a
- 43
44 500 Harrad, S.; Goosey, E.; Desborough, J.; Abdallah, M.A.-E.; Roosens, L.; Covaci, A.
45 501 Dust from U.K. Primary School Classrooms and Daycare Centers: The
46 502 Significance of Dust As a Pathway of Exposure of Young U.K. Children to
47 503 Brominated Flame Retardants and Polychlorinated Biphenyls. *Environmental*
48 504 *Science & Technology*. 44:4198-4202; 2010b
- 49
50 505 Harrad, S.; Ibarra, C.; Abdallah, M.A.-E.; Boon, R.; Neels, H.; Covaci, A.
51 506 Concentrations of brominated flame retardants in dust from United Kingdom
52 507 cars, homes, and offices: Causes of variability and implications for human
53 508 exposure. *Environment International*. 34:1170-1175; 2008
- 54
55 509 Jones-Otazo, H.A.; Clarke, J.P.; Diamond, M.L.; Archbold, J.A.; Ferguson, G.;
56 510 Harner, T.; Richardson, G.M.; Ryan, J.J.; Wilford, B. Is House Dust the
57 511 Missing Exposure Pathway for PBDEs? An Analysis of the Urban Fate and
58 512 Human Exposure to PBDEs. *Environmental Science & Technology*. 39:5121-
59 513 5130; 2005
- 60
61
62
63
64
65

1
2
3
4
5
6
7
8
9
10
11
12
13
14
15
16
17
18
19
20
21
22
23
24
25
26
27
28
29
30
31
32
33
34
35
36
37
38
39
40
41
42
43
44
45
46
47
48
49
50
51
52
53
54
55
56
57
58
59
60
61
62
63
64
65

514 Kajiwara, N.; Desborough, J.; Harrad, S.; Takigami, H. Photolysis of brominated
515 flame retardants in textiles exposed to natural sunlight. *Environmental*
516 *Science: Processes & Impacts*. 15:653-660; 2013
517 Keller, J.M.; Stapleton, H.M.; Heltsley, R.; Peck, A.; Kucklick, J.R.; Schantz, M.M.;
518 Wise, S.A. Standard reference materials available from the National Institute
519 of Standards and Technology for the analysis of brominated flame retardants.
520 Poster presented at BFR 2007; The Netherlands: Amsterdam. 2007
521 Rauert, C.; Lazarov, B.; Harrad, S.; Covaci, A.; Stranger, M. A review of chamber
522 experiments for determining specific emission rates and investigating
523 migration pathways of flame retardants. *Atmospheric Environment*. 48:44-55;
524 2014
525 Schripp, T.; Fauck, C.; Salthammer, T. Chamber studies on mass-transfer of di(2-
526 ethylhexyl)phthalate (DEHP) and di-n-butylphthalate (DnBP) from emission
527 sources into house dust. *Atmospheric Environment*. 44:2840-2845; 2010
528 Stapleton, H.; Harner, T.; Shoeib, M.; Keller, J.; Schantz, M.; Leigh, S.; Wise, S.
529 Determination of polybrominated diphenyl ethers in indoor dust standard
530 reference materials. *Analytical and Bioanalytical Chemistry*. 384:791-800;
531 2006
532 Suzuki, G.; Kida, A.; Sakai, S.-i.; Takigami, H. Existence State of Bromine as an
533 Indicator of the Source of Brominated Flame Retardants in Indoor Dust.
534 *Environmental Science & Technology*. 43:1437-1442; 2009
535 Wagner, J.; Ghosal, S.; Whitehead, T.; Metayer, C. Morphology, spatial distribution,
536 and concentration of flame retardants in consumer products and environmental
537 dusts using scanning electron microscopy and Raman micro-spectroscopy.
538 *Environment International*. 59:16-26; 2013
539 Webster, T.F.; Harrad, S.; Millette, J.R.; Holbrook, R.D.; Davis, J.M.; Stapleton,
540 H.M.; Allen, J.G.; McClean, M.D.; Ibarra, C.; Abdallah, M.A.-E.; Covaci, A.
541 Identifying Transfer Mechanisms and Sources of Decabromodiphenyl Ether
542 (BDE 209) in Indoor Environments Using Environmental Forensic
543 Microscopy. *Environmental Science & Technology*. 43:3067-3072; 2009
544

545 **Figures and Tables**

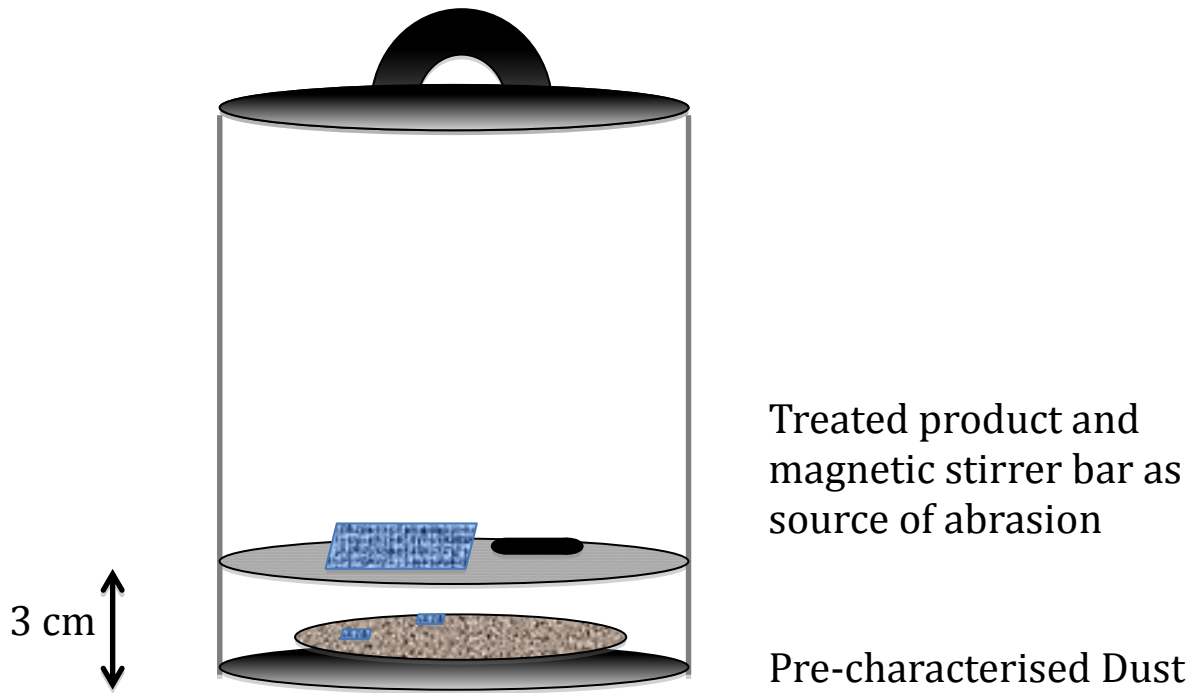
546

547 *Figure 1: Schematic of test chamber configuration for the abrasion induction*

548

experiments.

549



550

551

552

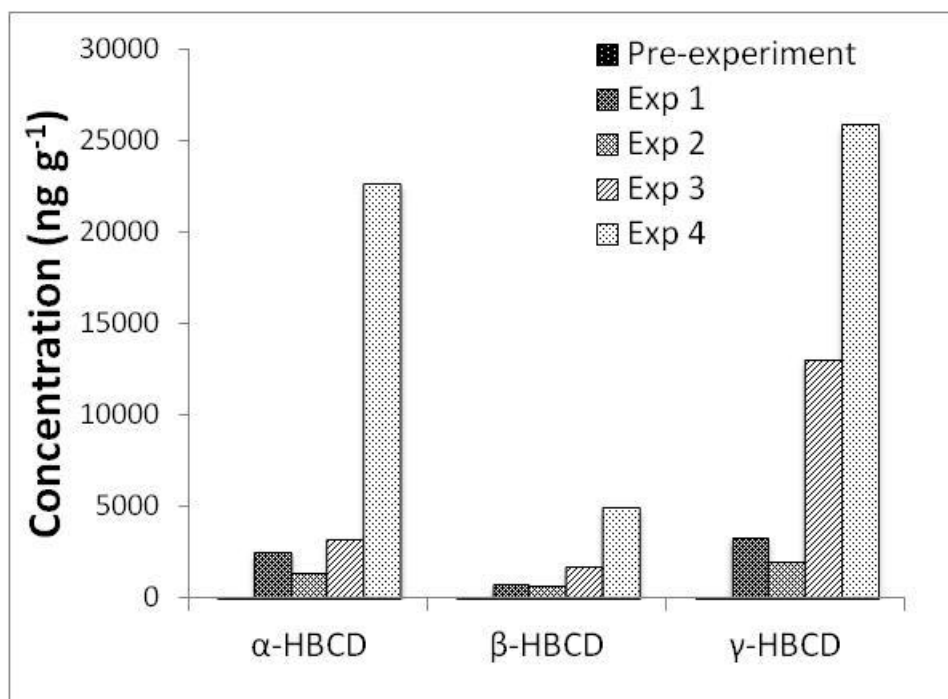
1
2
3
4
5
6
7
8
9
10
11
12
13
14
15
16
17
18
19
20
21
22
23
24
25
26
27
28
29
30
31
32
33
34
35
36
37
38
39
40
41
42
43
44
45
46
47
48
49
50
51
52
53
54
55
56
57
58
59
60
61
62
63
64
65

553

Figure 2: Concentration (ng g^{-1}) of HBCDs in dust both pre- and post-abrasion experiments ($n=4$)

554

555



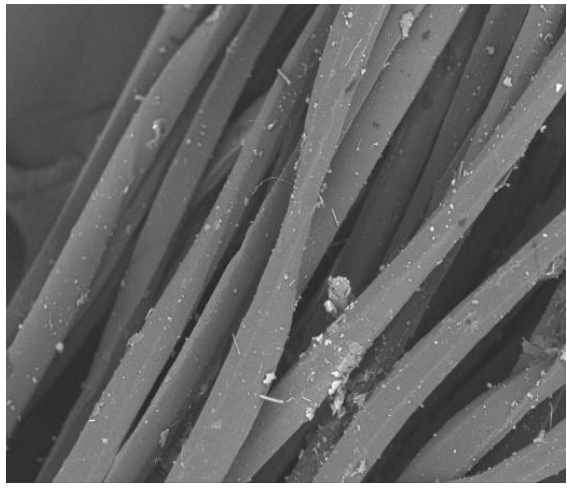
556

557

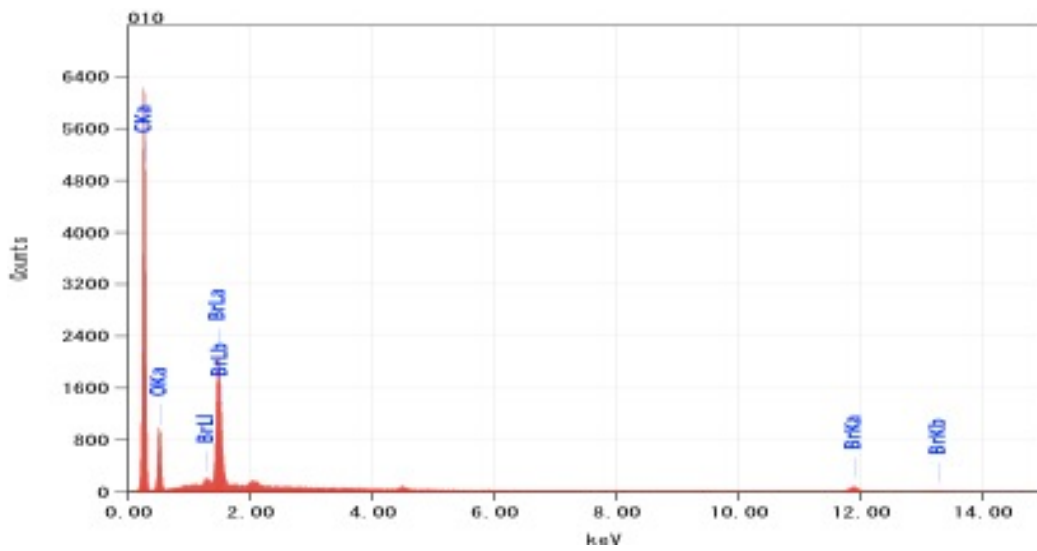
1
2
3
4
5
6
7
8
9
10
11
12
13
14
15
16
17
18
19
20
21
22
23
24
25
26
27
28
29
30
31
32
33
34
35
36
37
38
39
40
41
42
43
44
45
46
47
48
49
50
51
52
53
54
55
56
57
58
59
60
61
62
63
64
65

558
559
560

Figure 3: a) SEM backscattering image of fibres in post-abrasion induction experiment dust sample and b) EDS elemental profile in same fibres



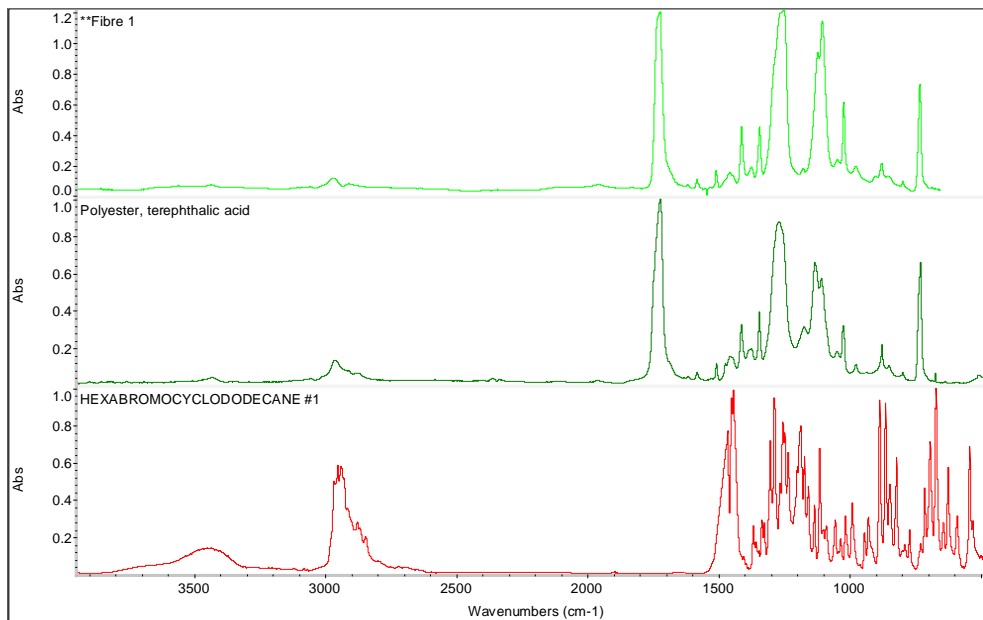
561
562



563
564

1
2
3
4
5
6
7
8
9
10
11
12
13
14
15
16
17
18
19
20
21
22
23
24
25
26
27
28
29
30
31
32
33
34
35
36
37
38
39
40
41
42
43
44
45
46
47
48
49
50
51
52
53
54
55
56
57
58
59
60
61
62
63
64
65

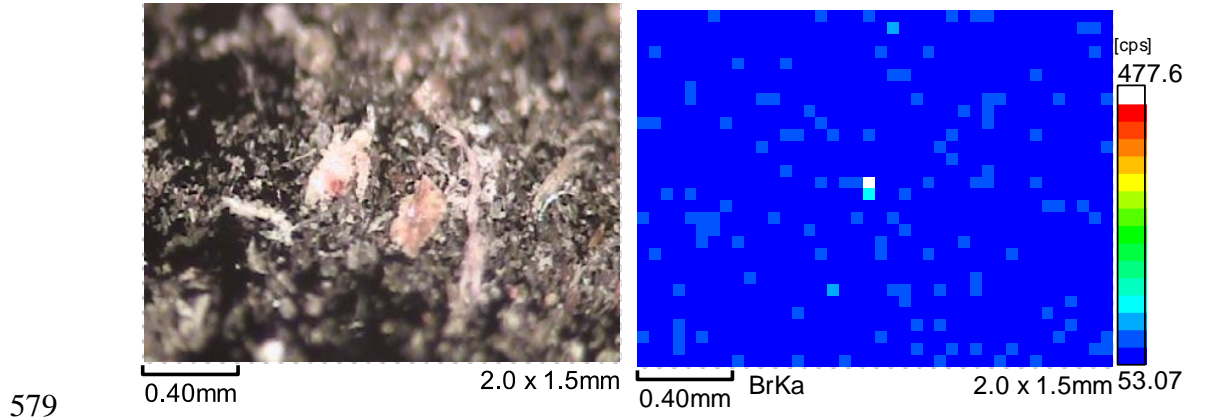
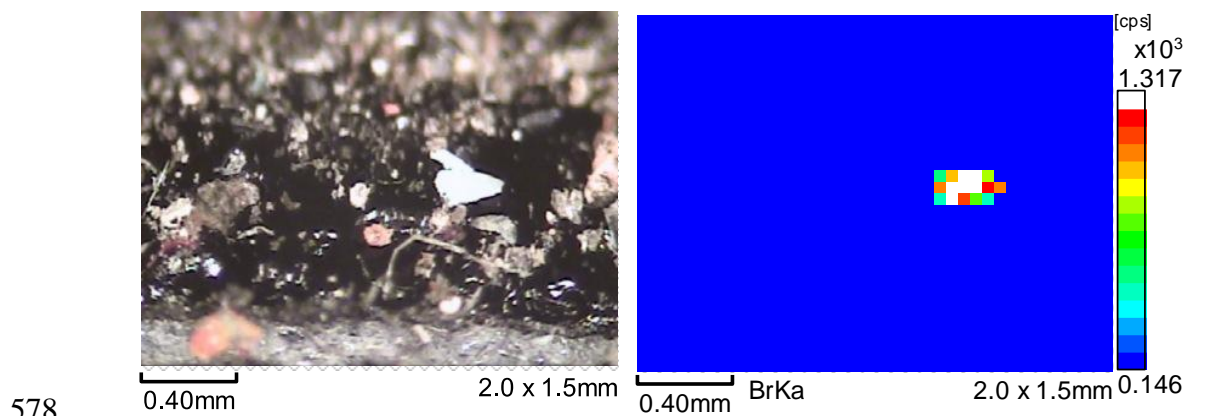
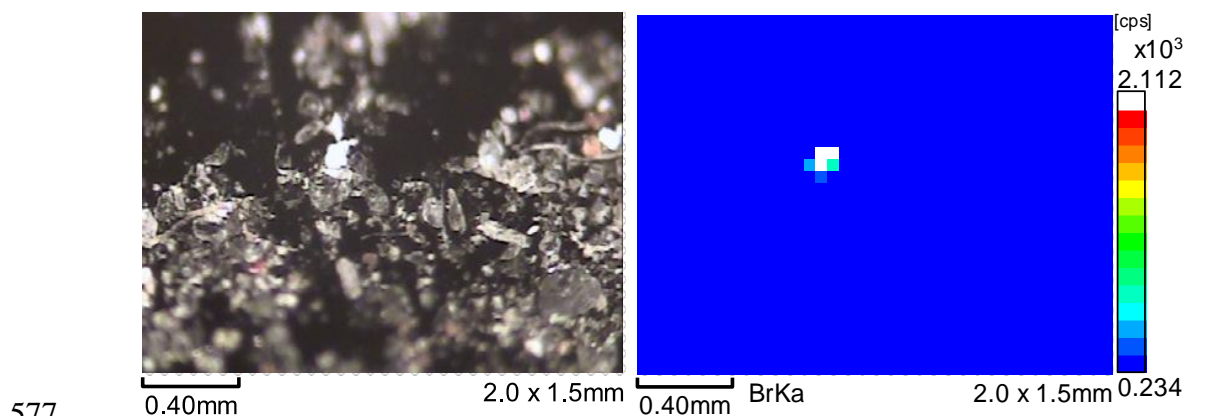
565 *Figure 4: FTIR spectra of a fibre isolated from a post-abrasion induction experiment*
566 *dust sample (top), with reference spectra for polyester (middle) and technical HBCD*
567 *(bottom)*



569
570

1
2
3
4
5
6
7
8
9
10
11
12
13
14
15
16
17
18
19
20
21
22
23
24
25
26
27
28
29
30
31
32
33
34
35
36
37
38
39
40
41
42
43
44
45
46
47
48
49
50
51
52
53
54
55
56
57
58
59
60
61
62
63
64
65

571 *Figure 5: Micro XRF images of areas/particles of high bromine content in dust*
 572 *samples containing elevated concentrations of BFRs:*
 573 *Images of areas in dusts 1,2 and 3 from top to bottom respectively.*
 574 *Left - Optical image of the mapped sample area and, Right - Bromine mapping image*
 575 *of the area, showing 50 μm square regions of high bromine in white/red/yellow*
 576



580

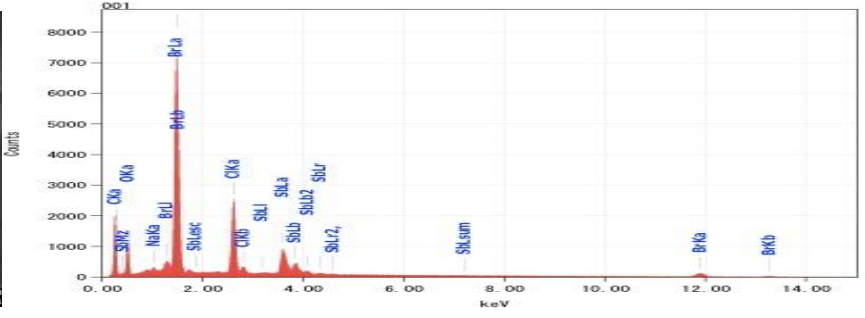
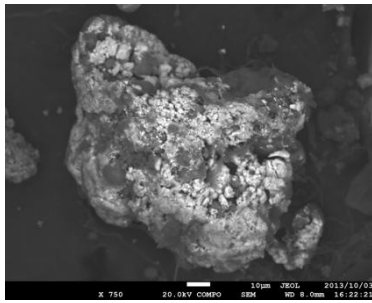
1
2
3
4
5
6
7
8
9
10
11
12
13
14
15
16
17
18
19
20
21
22
23
24
25
26
27
28
29
30
31
32
33
34
35
36
37
38
39
40
41
42
43
44
45
46
47
48
49
50
51
52
53
54
55
56
57
58
59
60
61
62
63
64
65

1
2
3
4
5
6
7
8
9
10
11
12
13
14
15
16
17
18
19
20
21
22
23
24
25
26
27
28
29
30
31
32
33
34
35
36
37
38
39
40
41
42
43
44
45
46
47
48
49

581 *Figure 6: From top to bottom, bromine rich particles in dusts 1,2 and 3 respectively: Left – Laser microscopy optical images of particles with*
582 *measured particle size. Right - SEM backscattering images of particles and related EDS elemental profiles.*



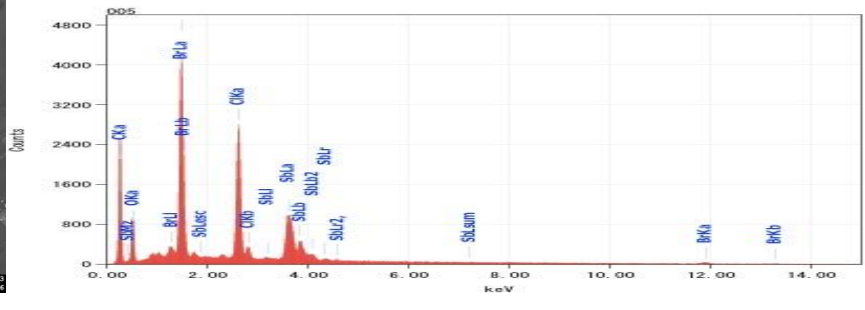
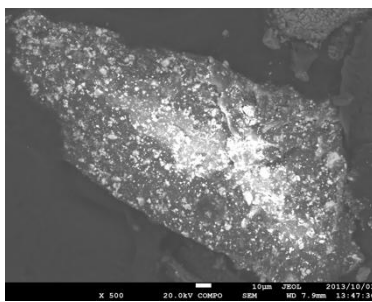
(120 µm)



583



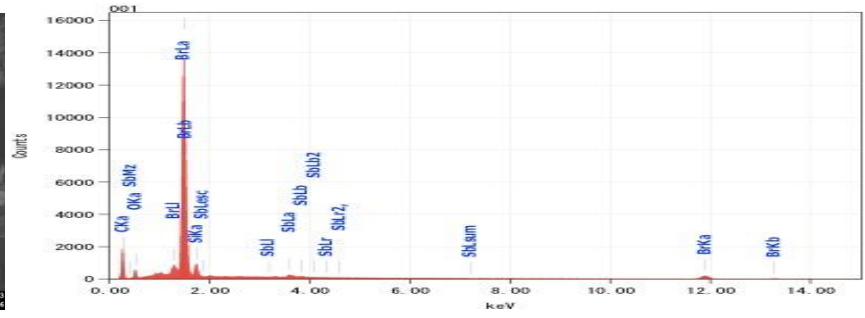
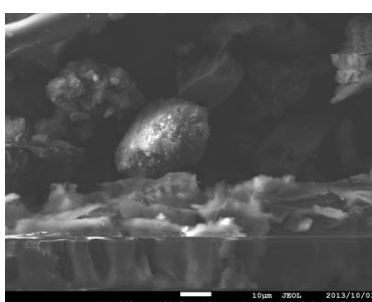
(260 µm)



584

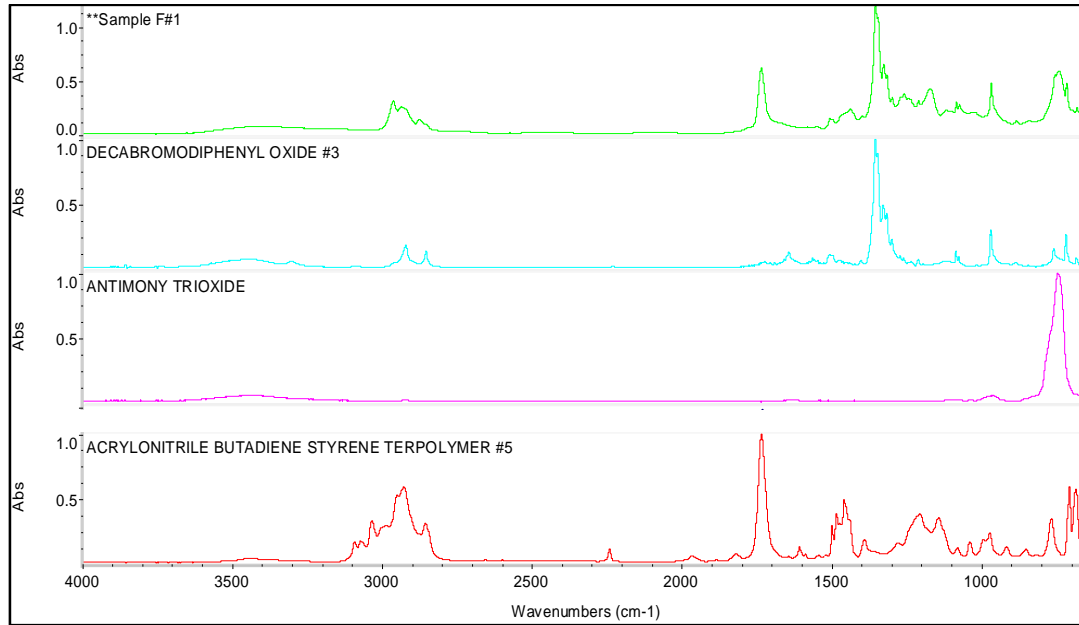


(35 µm)

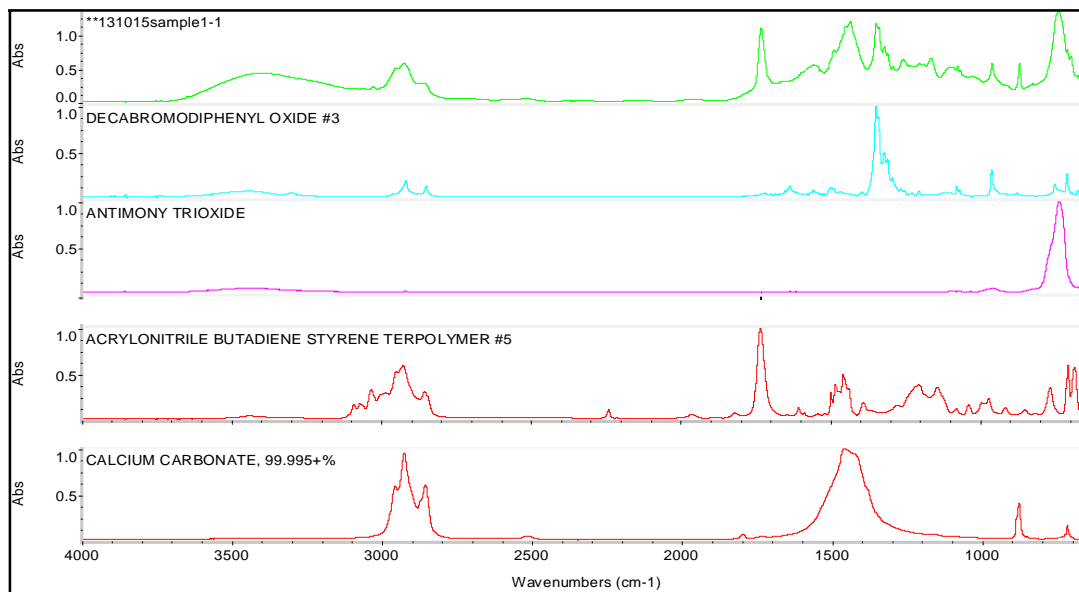


585

586 Figure 7: FTIR spectra of particles isolated from: Left - Dust 1 and Right - Dust 2,
587 featuring from top to bottom: dust sample, and reference spectra for BDE-209,
588 Antimony trioxide, ABS copolymer and (dust 2 only) calcium carbonate
589



590
591



592
593

1
2
3
4
5
6
7
8
9
10
11
12
13
14
15
16
17
18
19
20
21
22
23
24
25
26
27
28
29
30
31
32
33
34
35
36
37
38
39
40
41
42
43
44
45
46
47
48
49
50
51
52
53
54
55
56
57
58
59
60
61
62
63
64
65

594 *Table 1: Concentration (ng/g) of HBCDs and BDE-209 in archived dust samples*
 595 *(Harrad et al., 2010b; Harrad et al., 2008) and BDE-209 mass (ng) in combined*
 596 *isolated particles.*

	Concentration in bulk dust (ng g ⁻¹)				Mass in combined isolated particles (ng)
	α -HBCD	β -HBCD	γ -HBCD	BDE-209	BDE-209
Dust #1	380	340	2 800	1 438 000	500
Dust #2	280	70	140	280 000	1 300
Dust #3	9 900	6 700	72 000	24 000	N/A

598

599

1
2
3
4
5
6
7
8
9
10
11
12
13
14
15
16
17
18
19
20
21
22
23
24
25
26
27
28
29
30
31
32
33
34
35
36
37
38
39
40
41
42
43
44
45
46
47
48
49
50
51
52
53
54
55
56
57
58
59
60
61
62
63
64
65

600 *Supplementary Data*

601 *1.1 Sample preparation and extraction*

602 Sample extraction and purification was performed using slight modifications of in-
603 house published methods (Abdallah et al., 2009; Abdallah et al., 2008). Dust, PUFs
604 and GFFs were extracted with pressurised liquid extraction (ASE-350, Dionex Europe,
605 UK). PUFs and GFFs were packed into precleaned 66 mL cells using precleaned
606 Hydromatrix (Varian Inc., UK) to fill the void. Dust samples were loaded into pre-
607 cleaned 66 mL cells containing 1.5 g of pre-cleaned florisil and Hydromatrix. Each
608 cell was spiked with 4 ng each of ¹³C-labelled α-, β-, and γ-HBCD; 40 ng of ¹³C-
609 PBDE 47; 10 ng each of ¹³C-labelled PBDE-99 and PBDE-153; and 20 ng of ¹³C-
610 PBDE 209 as internal (surrogate) standards prior to extraction with
611 hexane:dichloromethane (1:1 v/v) at 90 °C and 1500 psi. The cell was heated for 5
612 min, held static for 4 min and purged for 90 s, with a flush volume of 50%, for 3
613 cycles.

614
615 *1.2 Clean up*

616 The ASE extracts and chamber inner surface solvent rinses were combined and
617 concentrated to 0.5 mL using a Zymark Turbovap II (Hopkinton, MA, USA), then
618 purified by loading onto SPE cartridges filled with 8 g of pre-cleaned acidified silica
619 (44% concentrated sulfuric acid, w/w). The analytes were eluted with 30 mL of
620 hexane:dichloromethane (1:1, v/v), with the eluate evaporated to dryness under a
621 gentle stream of nitrogen. Samples were reconstituted to 100 μL with 2 ng of d₁₈-γ-
622 HBCD and 20 ng of ¹³C-PBDE 100 in HPLC grade methanol, used as recovery
623 standards for internal standard recovery determination.

624
625 *1.3 LC-MS/MS analysis*

626 Target PBDEs and HBCDs were separated and analysed using modified, in-house
627 published methods (Abdallah et al., 2009; Abdallah et al., 2008), using a dual pump
628 Shimadzu LC-20AB Prominence liquid chromatograph (Shimadzu, Kyoto, Japan)
629 equipped with a SIL-20A autosampler, and a DGU-20A3 vacuum degasser. Mass
630 spectrometric analysis was performed using a Sciex API 2000 triple quadrupole mass
631 spectrometer (Applied Biosystems, Foster City, CA) equipped with an APPI (PBDEs)
632 or ESI (HBCDs) ion source, operated in negative ion mode.

633

634 *1.3.1 PBDE Analysis*

635 A Varian Pursuit XRS3 (Varian, Inc., Palo Alto, CA) C18 reversed phase analytical
636 column (250 mm x 4.6 mm i.d., 3 μm particle size) was used for separation of target
637 PBDEs (47, 85, 99, 100, 153, 154, 183 and 209). A mobile phase programme based
638 upon (mobile phase A) 1:1 methanol/water and (mobile phase B) 1:4
639 toluene/methanol at a flow rate of 0.4 mL min⁻¹ was applied for elution of the target
640 compounds; starting at 85% (mobile phase B), increased linearly to 100% (mobile
641 phase B) over 20 min, and then held for 10 min. The column was equilibrated with
642 85% (mobile phase B) for 5 min between runs. MS/MS detection, operated in MRM
643 mode, was used for quantitative determination of the PBDE congeners based on m/z
644 420.8 \rightarrow 78.8, m/z 500.8 \rightarrow 78.8, m/z 578.8 \rightarrow 78.8, m/z 658.6 \rightarrow 78.8, m/z 486.6 \rightarrow 78.8.
645 ¹³C-labelled analogues were determined based on m/z 432.4 \rightarrow 78.8, 512.4 \rightarrow 78.8,
646 590.6 \rightarrow 78.8, and m/z 494.7 \rightarrow 78.8.

647
648 *1.3.2 HBCD Analysis*

649 A Varian Pursuit XRS3 C18 reversed phase analytical column (150 mm x 4.6 mm i.d.,
650 3 μm particle size) was used for separation of target HBCDs (α -, β -, γ -). A mobile
651 phase program based upon (mobile phase A) 1:1 methanol/water and (mobile phase
652 B) methanol at a flow rate of 0.18 mL min⁻¹ was applied for elution of the target
653 compounds; starting at 50% (mobile phase B), then increased linearly to 100%
654 (mobile phase B) over 4 min, held for 5 min before decreasing linearly to 88%
655 (mobile phase B) over 1 min. The column was equilibrated with 50% (mobile phase
656 B) for 4 min between runs. MS/MS detection, operated in MRM mode, was used for
657 quantitative determination of the HBCD diastereomers, ¹³C-, and d₁₈-labelled
658 analogues based on m/z 640.4 \rightarrow 79.0, m/z 652.4 \rightarrow 79.0, and m/z 657.7 \rightarrow 79 respectively.

659 *1.4 Quality Assurance*

660 Samples were analysed using established QA/QC procedures. Method blanks were
661 run with each batch of samples. For ¹³C- α -, β -, and γ -HBCDs, average recoveries
662 ranged from 64 to 97% while for ¹³C-PBDE 47, 99, 153, and 209, average recoveries
663 ranged between 69 and 80%. Accuracy and precision of the analytical method was
664 assessed *via* replicate analyses (n=7) of NIST SRM 2585 (organics in house dust).
665 The results of these analyses compared with indicative and certified values as
666 appropriate are supplied in Table SD-1.

1
2
3
4
5
6
7
8
9
10
11
12
13
14
15
16
17
18
19
20
21
22
23
24
25
26
27
28
29
30
31
32
33
34
35
36
37
38
39
40
41
42
43
44
45
46
47
48
49

667 *Table SD-1: Average concentrations (ng g⁻¹) in 7 analyses of SRM 2585 and the reported certified PBDE (Stapleton et al., 2006) and indicative*
668 *HBCD values (Keller et al., 2007)*

	BDE-47	BDE-85	BDE-99	BDE-100	BDE-153	BDE-154	BDE-183	BDE-209	α-HBCD	β-HBCD	γ-HBCD
<i>SRM Measured Value (n=7)</i>	347 ± 39	35.1 ± 4.6	730 ± 93	133 ± 13	126 ± 13	78.6 ± 13	44.4 ± 5.0	2460 ± 400	19 ± 5.7	5.6 ± 2.2	98 ± 35
<i>Certified/Indicative Values</i>	498 ± 46	43.8 ± 1.6	892 ± 53	145 ± 11	119 ± 11	83.5 ± 2.0	43.0 ± 3.5	2510 ± 190	19 ± 3.7	4.3 ± 1.1	120 ± 22

670

Conflict of Interest Declaration

We wish to confirm that there are no known conflicts of interest associated with this publication and there has been no significant financial support for this work that could have influenced its outcome.

We confirm that the manuscript has been read and approved by all named authors and that there are no other persons who satisfied the criteria for authorship but are not listed. We further confirm that the order of authors listed in the manuscript has been approved by all of us.

We confirm that we have given due consideration to the protection of intellectual property associated with this work and that there are no impediments to publication, including the timing of publication, with respect to intellectual property. In so doing we confirm that we have followed the regulations of our institutions concerning intellectual property.

We understand that the Corresponding Author is the sole contact for the Editorial process (including Editorial Manager and direct communications with the office). He/she is responsible for communicating with the other authors about progress, submissions of revisions and final approval of proofs. We confirm that we have provided a current, correct email address which is accessible by the Corresponding Author and which has been configured to accept email from: c.b.rauert@bham.ac.uk

Signed by all authors as follows:


Cassandra Rauert

 13/3/14


Stuart Harrad

 13/3/14


Go Suzuki

 14/3/14

Hidetaka Takigami

 16/3/14

Natsuyo Uchida

 14/3/14

Kyouko Takata

 14/3/14